J Appl Electrochem (2007) 37:1183–1190
DOI 10.1007/s10800-007-9384-3

ORIGINAL PAPER

Effect of ascorbic acid on mild steel dissolution in sulphuric acid solution investigated by electrochemical polarization and surface probe techniques

E. E. Oguzie · Y. Li · F. H. Wang

Received: 2 March 2007 / Revised: 16 July 2007 / Accepted: 18 July 2007 / Published online: 15 August 2007

Abstract The effect of ascorbic acid (AA) on the corrosion of mild steel in sulphuric acid solution has been investigated by open circuit potential (OCP) and polarization measurements. AA was observed to shift the OCP to more positive potentials with increasing concentration. The polarization curves revealed that AA inhibited the anodic metal dissolution reaction, although this effect became negligible at high anodic overpotentials. The trend of inhibition efficiency with concentration showed that efficiency increased rapidly at low concentrations, remained almost steady at intermediate concentrations and increased again at high concentrations. The mechanism of inhibition was considered in terms of initial chemisorption of AA according to the Temkin isotherm, followed by formation of chelate compounds with Fe^{2+} ions at high concentrations. EDS and AFM analyses of the electrode surface support the proposed inhibition mechanisms.

Keywords Mild steel · Ascorbic acid · Chemisorption · Chelation · Surface morphology

E. E. Oguzie · Y. Li (✉) · F. H. Wang
State Key Laboratory for Corrosion and Protection,
Institute of Metal Research, Chinese Academy of Sciences,
62 Wencui Road, Shenyang 110016, China
e-mail: liying@imr.ac.cn

E. E. Oguzie
Electrochemistry and Materials Science Research Laboratory,
Department of Chemistry, Federal University of Technology
Owerri, PMB 1526, Owerri, Nigeria

1 Introduction

Organic compounds containing polar groups with nitrogen, sulphur and/or oxygen in a conjugated system are effective corrosion inhibitors for steel [1–11]. Corrosion inhibition by such compounds is generally attributed to their adsorption on the metal/solution interface. The specific action of an additive depends on the nature of its interaction with the metal surface, which causes a change in either the mechanism of the electrochemical corrosion process or in the surface area available for the process. Thus, factors such as the physicochemical properties of the additive, the nature and surface charge of the metal, solution composition and pH are important considerations.

The current focus on the development of environmentally friendly processes has led to increased interest in the assessment of natural products [12–15] and certain biochemical compounds [16–19] for corrosion inhibiting efficacy. Ascorbic acid (AA) belongs to a class of non-toxic, water soluble compounds whose molecules possess the desirable characteristics of a corrosion inhibitor (Fig. 1). It is a weak dibasic acid (pK_{a1} = 4.25, pK_{a2} = 11.79), but the monoanion, which forms at pH 4–5 with deprotonation of O(3)–H, is more stable due to the delocalization of the negative charge between the oxygen atoms in positions (1) and (3). The coordination chemistry of AA has been recently reviewed by Zumreoglu-Karan [20]. Interaction with metals occurs monodentately through the O(3) atom or more commonly by chelation via O(3) and O(2), depending on the nature of the metal ion, pH and solution concentration. Participation of the carbonyl oxygen and side chain OH groups has been proposed in the solid state. The ascorbic acid crystal is stable in air, but is rapidly air-oxidized in solution and gradually decomposes to dehydroascorbic acid (DHA), which is a more reactive, unstable

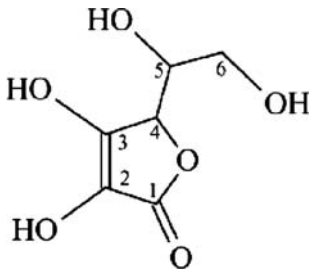

Fig. 1 L-Ascorbic acid

and less effective ligand [20, 21]. Further oxidation yields furoic acid and 3-hydroxy-2-pyrone, while furfural is produced under anaerobic conditions. The decomposition process is sensitive to solution pH, showing a maximum at pH 4.0 and a minimum at pH 2.5–3.0 [22]. Lyman et al. [21] reported that at pH ≤ 2, AA is only very slightly oxidized to DHA in sulphuric acid solution.

The inhibitive effect of AA on the corrosion of SS 41 alloy in 0.3% NaCl solution was reported by Sekine et al. [23], Nigam et al. [24] studied the effect on mild steel corrosion by brackish water, Goncalves and Mello [25] considered the adsorption of AA on low carbon steel in 0.5 M Na_2SO_4 solution, while Ferreira et al. [26] looked into the inhibiting effect of AA on mild steel containing 2.34% Cr, in acid sulphate solution. No such study has been reported with regard to mild steel corrosion in sulphuric acid solution. The significance of acid solutions lies in their widespread use in a number of industrial processes in which steel materials and structures are used. In the present study we have investigated the influence of ascorbic acid on the electrochemical polarization and corrosion behaviour of mild steel in 0.5 M sulphuric acid. Surface analytical examinations of the steel specimens were undertaken by energy dispersive spectroscopy (EDS) and atomic force microscopy (AFM).

2 Experimental

Tests were performed on mild steel specimens of the following percentage composition (C: 0.22; Si: 0.1–0.3; Mn: 0.6; P: 0.045). This was machined into test electrodes of dimensions 1 × 1 × 2 cm and fixed in polytetrafluoroethylene (PTFE) rods by epoxy resin in such a way that only one surface of area 1 cm^2 was left uncovered. The exposed surface was wet-polished with silicon carbide abrasive paper (from grade #200 to #1000), degreased in acetone, rinsed with distilled water and dried in warm air. The aggressive solution was 0.5 M H_2SO_4 solution, prepared from analytical reagent grade sulphuric acid and distilled water. L-Ascorbic acid (AA) was obtained from (SCRC, China) and dissolved in 0.5 M H_2SO_4 solution to obtain the desired concentration (0.05–10 mM).

Electrochemical polarization experiments were conducted in a conventional three-electrode glass cell of 400 mL capacity using an AUTOLAB PGSTAT 30 potentiostat/galvanostat (Eco Chemie BV, Netherlands) equipped with General Purpose Electrochemical System (GPES 4.9) software. A platinum foil was used as counter electrode and a saturated calomel electrode (SCE) as reference electrode. The latter was connected via a Luggin capillary. The variation of the open circuit potential (OCP) of mild steel with time in the different solutions was followed for 2 h. Electrochemical polarization studies were carried out after OCP tests, when the potential had reached a steady value, in the potential range ±250 mV vs. corrosion potential (E_{corr}) at a scan rate of 0.33 mV s^{-1}. Measurements were made in aerated solutions under static conditions at a fixed temperature of 30 ± 1 °C. Tests in the presence of 0.1 and 5.0 mM AA were also repeated under deaerated conditions, where the test solutions were bubbled with a stream of nitrogen for 30 min prior to electrode immersion and during OCP and polarization measurements. Each test was run in triplicate to verify the reproducibility of the results.

SEM-EDS analyses of electrode surfaces exposed to different test solutions for 2 h were achieved using a Shimadzu SSX-550 scanning electron microscope while AFM morphological images were realized in tapping mode at room temperature using a PicoPlus Scanning Probe Microscope.

3 Results and discussion

3.1 Open circuit potential measurements

The evolution of the open circuit potential (OCP) with time for mild steel in 0.5 M H_2SO_4 solution without and with different concentrations of AA (0.05–5.0 mM) is illustrated in Fig. 2. A gradual positive displacement of potential with time is observed for all the curves after an initial sharp decrease due to dissolution of the electrode oxide film. Compared to the blank solution, a positive shift of corrosion potential is observed with increasing AA concentration, indicating anodic polarization. OCP values after 2 h immersion period increased from –525 mV in the blank acid to –517 mV in 0.05 mM AA and –454 mV in 5 mM AA.

3.2 Polarization measurements

Mild steel dissolution in acidic solutions commences with generation of ferrous ions by anodic oxidation at the steel/solution interface due to the reaction:

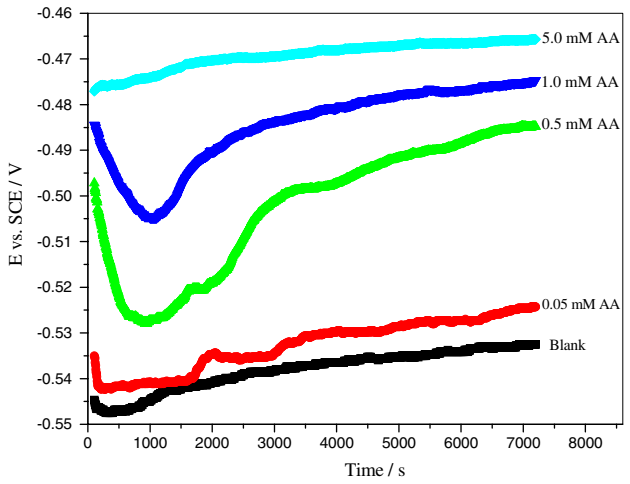

Fig. 2 Variation of open circuit potential (OCP) with time for mild steel in 0.5 M H_2SO_4 without and with different concentrations of AA

$$\mathrm{Fe} \rightarrow \mathrm{Fe}^{2+} + 2\mathrm{e} \tag{1}$$

The cathodic process is controlled by the proton discharge step of the hydrogen evolution reaction

$$2\mathrm{H}^{+} + 2\mathrm{e} \rightarrow \mathrm{H}_2 \tag{2}$$

Figure 3a, b show the anodic and cathodic polarization curves for mild steel in aerated 0.5 M H_2SO_4 in the absence and presence of different AA concentrations. The plots indicate that the anodic and cathodic reactions in blank acid follow Tafel's law and the related current densities correspond to [27]:

$$I_a = k_a \exp(E/\beta_a); \quad I_c = -k_c(-E/\beta_c) \tag{3}$$

E is any metal/solution potential, the direction of the cathodic reaction is taken as negative and I_c is a negative value. In the presence of 0.05–0.1 mM AA (Fig. 3a), E_{corr} is shifted a little in the anodic direction and a slight inhibiting effect is observed on the anodic reaction while the cathodic reaction is not notably affected. The presence of 0.5–10 mM AA (Fig. 3b) produced more pronounced effects. A considerable displacement of E_{corr} in the anodic direction is observed and the anodic reaction is significantly inhibited.

It is generally assumed that the first step in the action mechanism of an organic inhibitor in acid solution is adsorption on the metal/solution interface by replacing one or more of the adsorbed water molecules [28]:

$$\mathrm{AA}_{(\mathrm{sol})} + x\mathrm{H_2O}_{(\mathrm{ads})} \rightleftharpoons \mathrm{AA}_{(\mathrm{ads})} + \mathrm{H_2O}_{(\mathrm{sol})} \tag{4}$$

The rates of the anodic and cathodic reactions in the presence of an adsorbed inhibitor can then be described by [29]:

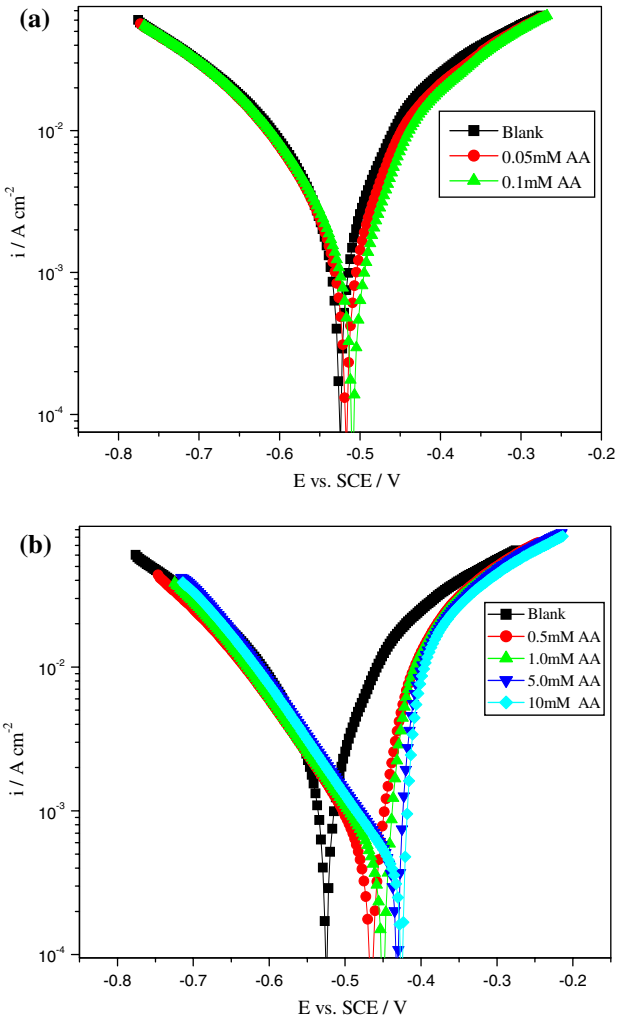

Fig. 3 Polarization curves of mild steel in 0.5 M H_2SO_4 in the absence and presence of (**a**) 0.05–0.1 mM AA and (**b**) 0.5–10 mM AA

$$i_a = k_a(1-\theta)\exp\left[\frac{F}{RT}z\beta(E-\Psi_1)\right] \tag{5}$$

$$i_c = [\mathrm{H_3O^+}](1-\theta)\exp\left\{\frac{F}{RT}[\alpha E + (1-\alpha)\Psi_1]\right\} \tag{6}$$

where k_a and k_c are the corresponding rate constants, θ the fraction of electrode surface covered by adsorbed inhibitor, E is the electrode potential relative to the solution potential, Ψ_1 is the potential drop in the outer part of the double layer, α and β are the symmetry factors for both reactions and z is the charge of the metal ion in solution. The adsorbed inhibitor, depending on its specific properties can influence the corrosion reaction by either geometrical blocking of the electrode surface, thereby restricting the access of corrosive species to, or transfer of corrosion products away from it, or by blocking and deactivating the active reaction sites on the electrode. One way to ascertain

the predominant mechanism, although not conclusively, is by considering the shift in corrosion potential (ΔE_{corr}) produced by the inhibitor:

$$\Delta E_{corr} = E'_{corr} - E_{corr} = \beta_a\beta_c/(\beta_a + \beta_c)\ln(f_a/f_c)_{E'_{corr}} \quad (7)$$

According to Cao [27] f_a and f_c are the action coefficients of the inhibitor on the anodic and cathodic reactions, respectively, which at any given potential are related to the current densities in the absence (I) and presence (I') of inhibitor by [$I_a' = f_a I_a$ and $I_c' = f_c I_c$]. Our experimental results for AA indicate that $f_a < 1$ over a wide potential range and f_c approaches unity. For an inhibitor that functions by the geometric blocking effect, $f_a \approx f_c$ and ΔE_{corr} 0, i.e., the shift in E_{corr} will not be significant. On the other hand, if inhibition is due to deactivation of active surface sites, $f_a \neq f_c$ and the outcome will be a significant shift in E_{corr}. From Figs. 3, 4 it is obvious that for [AA] ≤ 0.1 mM ΔE_{corr} is only marginal, but for [AA] ≥ 0.5 mM ΔE_{corr} becomes appreciable, suggesting dissimilar inhibition mechanisms at low and high concentrations.

The polarization curves obtained in deaerated solution in the presence of AA at low (0.1 mM) and high (5.0 mM) concentrations are compared with those in aerated solution in Fig. 4. The results show that the presence of oxygen in the solution containing a low concentration of AA (Fig. 4a) led to a negative shift of E_{corr} and slightly increased the anodic and cathodic reaction rates at low overpotentials. This may be related to permeability of the AA film which permits oxygen diffusion from the bulk solution to the electrode surface [30]. This effect becomes unimportant at higher AA concentrations, where the interaction between the inhibitor and the steel electrode was not significantly affected by the presence of oxygen (Fig. 4b) probably because the inhibitor film is more compact. A similar observation was reported for 10 mM AA [25].

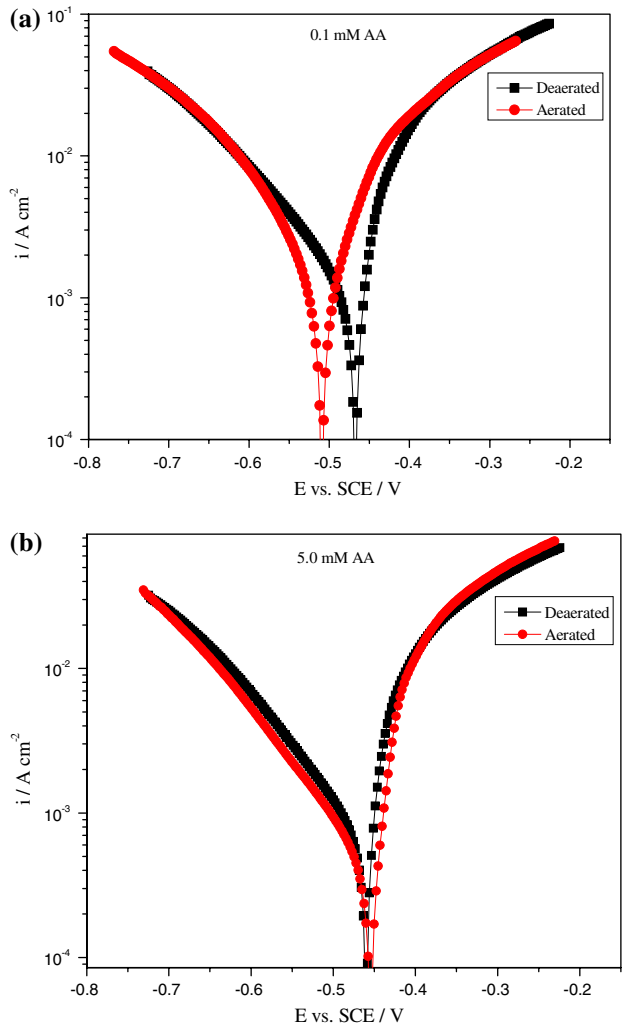

Fig. 4 Polarization curves of mild steel in aerated and deaerated 0.5 M H_2SO_4 containing (**a**) 0.1 mM AA and (**b**) 5.0 mM AA

3.3 Inhibition mechanism

Polarization resistances, R_p, for mild steel in 0.5 M H_2SO_4, without and with AA, were determined from the polarization curves in the vicinity of $E_{corr.}$ R_p values were used to calculate the inhibition efficiency (η_R%) of AA at different concentrations by [$\eta_R\% = (1 - R_p/R_p') \times 100$], where R_p is the polarization resistance value in 0.5 M H_2SO_4 solution without AA and R_p' is the polarization resistance in the presence of AA. The values of R_p and η_R% are plotted in Fig. 5 as a function of AA concentration. The polarization resistance is observed to become higher in the presence of AA, indicating an inhibiting effect, and generally increased with AA concentration. Inhibition efficiency also increased with AA concentration, displaying three distinct regions at low, intermediate and high concentrations.

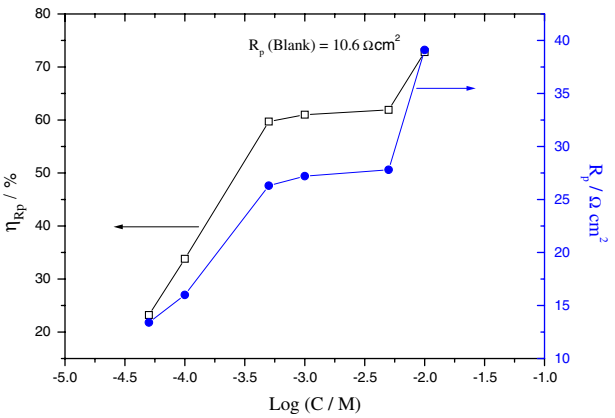

Fig. 5 Variation of polarization resistance (R_p) and inhibition efficiency (η%) with logarithmic concentration of AA

The polarization curves in the presence of AA (Fig. 3) show that the anodic polarization was more pronounced than the cathodic polarization, indicating that the corrosion process was under anodic control. At high concentrations, AA is observed to exert a slight depolarizing action on the cathodic process at potentials more positive than E_{corr} in the blank acid, which is in agreement with the results of the OCP measurements. The reason for this depolarizing action is not clear, but, as suggested in [25], could be related to possible stimulation of the cathodic process by adsorbed corrosion products from AA electroreduction. The anodic inhibition mechanism suggested by the polarization results agrees well with the findings of Sekine et al. [23] and Goncalves and Mello [25] for the inhibiting effect of AA on steel corrosion in 0.3 M NaCl and 0.5 M Na_2SO_4 solutions, respectively. Nigam et al. [24] also reported that the presence of AA in brackish water drastically affected the chemical process of steel corrosion and suppressed the formation of the usual corrosion species such as β,γ-FeO-OH and ferrihydrite ($FeCl_2{\cdot}4H_2O$), thus retarding the rate of rust formation.

The anodic process mechanism is seen to depend on AA concentration as well as the applied potential. At potentials more negative than –0.3 V, the anodic process depends almost entirely on AA concentration, but is almost independent of concentration at more positive potentials (>–0.3 V) where the magnitude of the anodic current approaches that in the blank acid. The potential dependence of the protective action of AA is better illustrated in Fig. 6, which compares the extent of anodic polarization at different anodic potentials (–0.44, –0.41 and –0.35 V). Since the corrosion rate in each system is directly related to the magnitude of the current density, the inhibition efficiencies $\eta_I\%$, calculated at each stated potential by [$\eta_I\% = (1 - i_a'/i_a) \times 100$], are also included, where i_a' and i_a are the current densities in the presence and absence of AA. A more remarkable influence of AA (highest $\eta_{Ia}\%$) is observed at the least positive potential (–0.44 V) for all AA concentrations. As the potential becomes more positive the extent of polarization by AA decreases either due to restricted adsorption or desorption of adsorbed inhibitor.

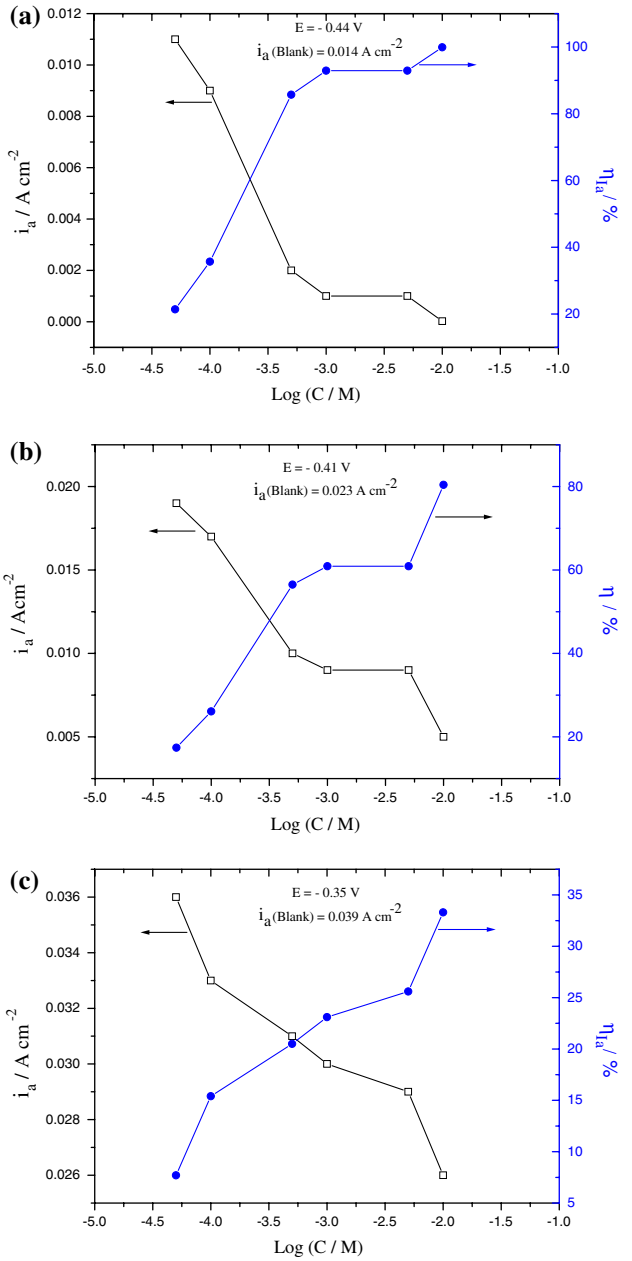

Fig. 6 Potential dependence of the anodic polarization of mild steel in 0.5 M H_2SO_4 by AA. (**a**) –0.44 V, (**b**) –0.41 V and (**c**) –0.35 V

3.4 Adsorption considerations

Basic information on the interaction between an organic inhibitor and a corroding metal surface can often be provided by the adsorption isotherm, which depends on the degree of electrode surface coverage, θ, [$\eta\% = \theta \times 100$]. As observed earlier, three distinct regions describe the concentration dependence of $\eta\%$ (Fig. 5). The initial region (0.05–0.5 mM AA) is characterized by a steep increase in $\eta\%$ with AA concentration, followed by a region (0.5–5.0 mM AA) where $\eta\%$ remains approximately constant while the third region ([AA] > 5.0 mM) again corresponds to an increase in $\eta\%$. These phenomena are related to changes in the thickness, the morphology and the composition of the protective film formed on the metal surface at different AA concentrations. The type of adsorption in the initial region was found to obey the Temkin adsorption isotherm, which characterizes the chemisorption of uncharged molecules on a heterogeneous surface. Figure 7 shows the plot of θ vs. log C to be linear, which is in agreement with the Temkin equation [30]:

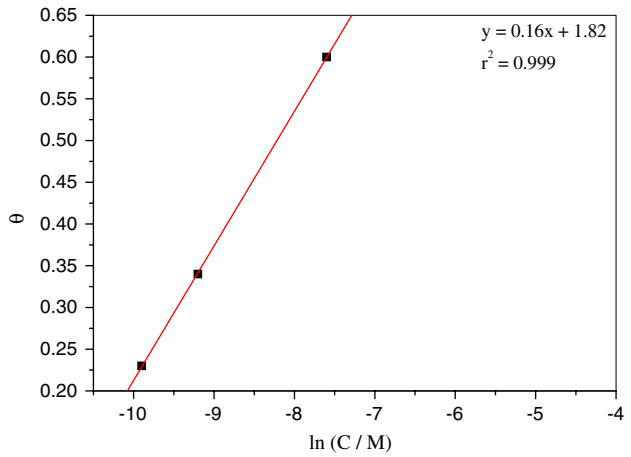

Fig. 7 Temkin isotherm for AA adsorption on mild steel in 0.5 M H_2SO_4 solution

$$\theta = (1/f)\ln K_{ads}C \tag{8}$$

where f is a factor of energetic inhomogeneity in the surface, C the adsorbate concentration and K_{ads} is the equilibrium constant for the adsorption process. The adsorption free energy ($\Delta G°$) obtained from the Temkin plot is about –38.76 kJ mol^{-1}, suggesting a chemically adsorbed film. The relative constancy of $\eta\%$ in the intermediate region indicates a constant activity of AA in the solution, whereas the increase in $\eta\%$ observed in the third region suggests that a more compact and effective protective film forms on the steel surface at [AA] > 5 mM. This could imply either the formation of a second layer of adsorbed inhibitor (bi-layer film) or formation of $[Fe\text{-}AA]^{2+}$ chelate compounds. Considering that AA predominantly functions as a chelating agent with transition metal ions [20], the latter effect is more probable. We thus attribute the steadiness in the effect of AA at intermediate concentrations to possible commencement of chelation between AA and freshly generated Fe^{2+} ions on the electrode surface while the increase in $\eta\%$ at higher concentration points towards a greater inhibiting effect of the resulting $[Fe\text{-}AA]^{2+}$ chelate. The proposed formation of $[Fe\text{-}AA]^{2+}$ chelates on the corroding mild steel surface at high AA concentrations has also been advocated by other authors, although considerable deviations exist in the reported functions of the resulting chelate compounds. Sekine et al. [23] reported such chelate formation at [AA] > 200 ppm in 0.3% NaCl, whereas Nigam et al. [24] observed chelation at [AA] ≥ 0.05 M in brackish water. In the former case, the formation of chelate compounds led to a marked decrease in the inhibiting effect of AA, while in the latter case the opposite effect corresponding to an increase in inhibition effectiveness due to chelation was observed. Such discrepancies can be correlated to the chemical stability of AA in the respective media.

As pointed out earlier, AA is easily oxidized in solution, in a pH-dependent mode, to DHA which is a less stable and less effective ligand than AA. The proportion of AA/DHA in solution will therefore influence the stability of the resulting chelate compound, i.e., the higher the rate of oxidation of AA to DHA, the less stable the resulting chelate and vice versa. Although experimental evidence of the AA/DHA ratio in 0.5 M H_2SO_4 solution is not presented, the improved $\eta\%$ obtained in the third region is indicative of a high stability of the resulting chelate compound, which is associated with a higher proportion of AA in solution. This is in agreement with the report of Lyman et al. [21] that at pH ≤ 2, AA is only slightly oxidized to DHA in sulphuric acid solution. From the foregoing, the proposed mechanism for the inhibiting action of AA involves initial chemisorption of AA and subsequent chelate formation. The structure of the chelate compound formed between ferrous ions and AA has not been conclusively determined. However, the available information suggest the existence of a high spin Fe^{2+} ion in a distorted octahedral environment, which can only be realized in a polymeric structure in which the ascorbate dianions use all their oxygen atoms as donor atoms, except that of the lactone ring [20, 24].

3.5 Surface morphological examination

The surface morphologies of steel specimen dipped in different test solutions were examined using a number of surface analytical techniques. EDS analysis was undertaken to verify the proposed existence of a corrosion inhibiting AA film on the steel surface. EDS spectra were used to determine the elements present on the electrode surface before and after exposure to the inhibitor solution. The spectra obtained in the blank acid showed some of the characteristic peaks of the elements present in the mild steel sample (Fe, C, Si, P) as well as S and O from the corrosion product. The spectra in the presence of AA did not show any additional peaks; rather the C and O signals were significantly enhanced, seemingly at the cost of the signals from the usual Fe corrosion species. For instance the peak intensity of the C signal (0.27 keV) and O signal (0.52 keV) increased from 0.346 and 0.421, respectively, in the blank acid to 0.656 and 12.32 in the presence of 5.0 mM AA. This shows that the surface contains additional carbon and oxygen atoms due to the presence of AA and is related to the carbon and oxygen content of the adsorbed AA film on the electrode surface. In addition, the Fe peaks (0.70 and 6.41 keV) decreased from 6.87 and 6.11, respectively, to 2.12 and 0.63, indicating a reduction in the corrosion rate.

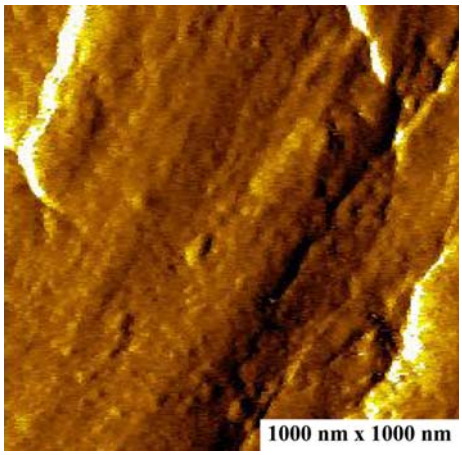

Fig. 8 AFM image of the as-received mild steel surface after polishing

The AFM topographic image of the mild steel surface before corrosion testing (Fig. 8) displays a regular relatively homogeneous surface with some imperfections due to the polishing treatment. The AFM phase images of mild steel specimens after 2 h immersion in 0.5 M H_2SO_4 without and with 0.1 and 5.0 mM AA are illustrated in Fig. 9. A severely corroded surface morphology is observed after immersion in the blank acid (Fig. 9a). Corrosion was relatively general with no evidence of localized attack. With addition of 0.1 mM AA (Fig. 9b) the corrosion rate is visibly reduced and there is slight evidence of inhibitor presence on the electrode surface. At higher concentration ([AA] = 5.0 mM), the corrosion rate is much reduced and a unique and even phase morphology is also produced, with small bead-like particles covering parts of the steel surface (Fig. 8c). Such a distinct and highly ordered film is not found in the corresponding image at low AA concentration and is related to the proposed formation of a chelate compound on the electrode surface at high AA concentrations. This is evidence that AA inhibited the corrosion reaction by different mechanisms at low and high concentration.

4 Conclusions

Ascorbic acid functioned as an anodic inhibitor for mild steel in 0.5 M H_2SO_4 solution and repressed the corrosion process at low concentrations (0.05–0.5 mM) by chemical adsorption according to the Temkin isotherm, but maintained a constant activity at intermediate concentrations (0.5–5.0 mM) due to commencement of chelation reaction with Fe^{2+} ions The inhibiting effect increased at high AA concentrations (>5.0 mM) due to improved surface coverage by the ensuing chelate compound. AA demonstrated an inhibiting effect at low anodic overpotentials but had negligible effect in the high overpotential region.

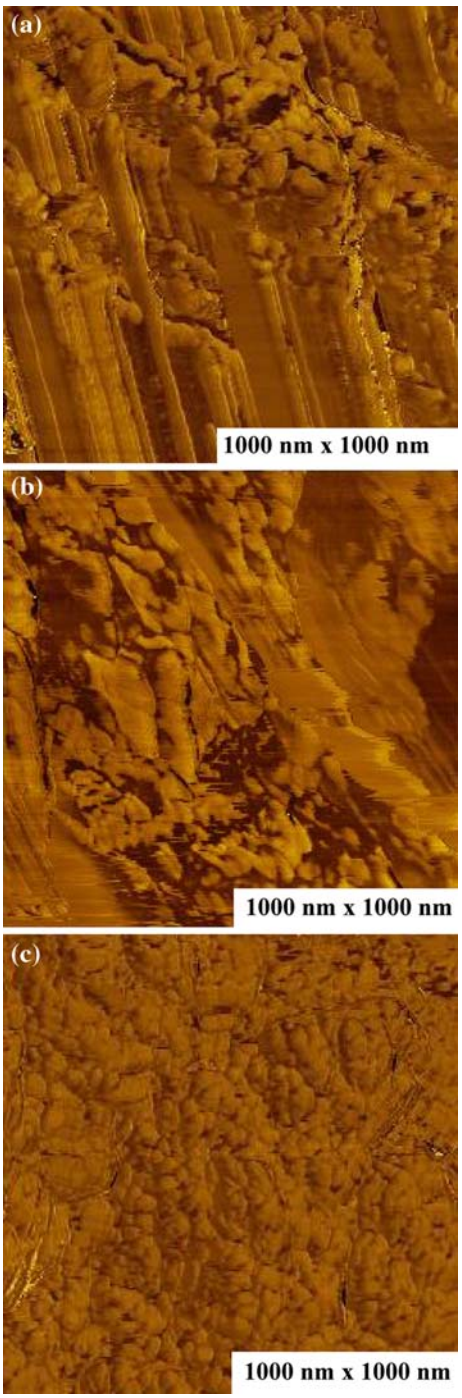

Fig. 9 AFM phase images of mild steel surfaces after 2 h exposure in 0.5 M H_2SO_4 solution (**a**) without inhibitor, (**b**) with 0.1 mM AA and (**c**) with 5.0 mM AA

Acknowledgements E. E. Oguzie is grateful to the Chinese Academy of Sciences (CAS) and the Academy of Sciences for the Developing World (TWAS) for the award of CAS-TWAS Fellowship.

References

1. Shibli SMA, Saji VS (2005) Corros Sci 47:2213
2. Mu G, Li X (2005) J Coll Interface Sci 289:184
3. Oguzie EE, Onuoha GN, Onuchukwu AI (2004) Mater Chem Phys 89:305
4. Oguzie EE, Unaegbu C, Ogukwe CN, Okolue BN, Onuchukwu AI (2004) Mater Chem Phys 84:363
5. Oguzie EE, Onuoha GN, Onuchukwu AI (2004) Mater Chem Phys 89:305
6. Harek Y, Larabi L (2004) Kem Ind 53(2):55
7. Kissi M, Bouklah M, Hammouti B, Benkaddour M (2006) Appl Surf Sci 252:4190
8. Ameer MA, Khamis E, Al-Senani G (2000) Ads Sci Tech 18(3):177
9. Christov M, Popova A (2004) Corros Sci 46:1613
10. Ateya BG, El-Anadouli BE, El-Nizamy FMA (1981) Bull Chem Soc Jpn 54:3517
11. Jianguo Y, Lin W, Otieno-Alego V, Schweinsberg DP (1995) Corros Sci 37(6):975
12. Oguzie EE (2006) Mater Chem Phys 99:441
13. Oguzie EE (2005) Pigmt Res Tech 34:321
14. Oguzie EE, Iyeh KL, Onuchukwu AI (2006) Bull Electrochem 22(2):63
15. Gunasekaran G, Chauhan LR (2004) Electrochim Acta 49:4387
16. Morad MS, El-Hagag A, Hermas A, Abdel Aal MS (2002) J Chem Technol Biotechnol 77:486
17. Moretti G, Guidi F, Grion G (2004) Corros Sci 46:387
18. Ochoa N, Moran F, Pebere W, Tribollet B (2005) Corros Sci 47:593
19. Matos JB, Pereira LP, Agostinho SML, Barcia E, Cordeiro GGO, D'Elia E (2004) J Electroanal Chem 570:91
20. Zumreoglu-Karan B (2006) Coord Chem Rev 250:2295
21. Lyman CM, Schultze MO, King CG (1937) J Biol Chem 113:757
22. Roig MG, Rivera ZS, Kennedy JF (1995) Int J Food Sci Nutr 46:107
23. Sekine I, Nakahata Y, Tanabe H (1988) Corros Sci 28:987
24. Nigam AN, Tripathi RP, Jangid ML, Dhoot K, Chacharkar MP (1990) Corros Sci 30:201
25. Goncalves RS, Mello LD (2001) Corros Sci 43:457
26. Ferreira ES, Giacomelli C, Giacomelli FC, Spinelli A (2004) Mater Chem Phys 83:129
27. Cao C (1996) Corros Sci 38:2073
28. Bockris JO, Swinkels DAJ (1964) J Electrochem Soc 11:736
29. Popova A, Sokolova E, Raicheva S, Christov M (2003) Corros Sci 45:33
30. Chikh ZA, Chebabe D, Dermaj A, Hajjaji N, Srhiri A, Montemor MF, Ferreira MGS, Bastos AC (2005) Corros Sci 47:447